Decoding the Cure-all Effects of Ginseng

Shining Loo[1,2,‡], Antony Kam[1,3,‡], Bamaprasad Dutta[1], Xiaohong Zhang[1], Nan Feng[4], Siu Kwan Sze[1,5], Chuan-Fa Liu[1], Xiaoliang Wang[1,4], and James P. Tam[1]*

[1] School of Biological Sciences, Nanyang Technological University, 60 Nanyang Drive, Singapore 637551
[2] Academy of Pharmacy, Xi'an Jiaotong-Liverpool University, Suzhou, 215123, China.
[3] Department of Biological Sciences, Xi'an Jiaotong-Liverpool University, Suzhou 215123, China
[4] Institute of Materia Medica, Chinese Academy of Medical Sciences, Beijing 100050, China
[5] Department of Health Sciences, Brock University, Niagara Region,1812 Sir Isaac Brock Way, St. Catharines, ON L2S 3A1

KEYWORDS. Ginseng; cysteine-rich peptides; microproteins; Cure-all; stress homeostasis

Abstract

Ginseng has been known as a "cure-all" traditional medicine to treat various illnesses and as an adaptogen to relieve stress. However, the known active compounds of ginseng are small-molecule metabolites. Here we report ginsentides, which are disulfide-dense, super-stable and cell-penetrating peptides with 31–33 amino acids, as active compounds and adaptogens that restore homeostasis in response to stress. Using mass spectrometry-based target identification and functional studies, we show that ginsentides promote vasorelaxation by producing nitric oxide through endothelial cells via the PI3K/Akt signaling pathway. Ginsentides were also found to alleviate α1-adrenergic receptor overactivity by reversing phenylephrine-induced constriction of the aorta, decrease monocyte adhesion to endothelial cells via CD166/ESAM/CD40, inhibit P2Y12 receptors, reduce platelet aggregation, and thrombus formation in the lung. Orally administered ginsentides were effective in anti-stress behavior using animal models of tail suspension and forced swimming tests. Together, these results suggest that ginsentides interact with multiple systems to restore homeostasis by reversing stress-induced physiological changes and provide new insights into the panacea medicinal effects of ginseng.

33 **Introduction**

34 Ginseng is a popular traditional medicine with a wide range of pharmacological
35 effects and a long history of usage for health maintenance and treatment of diseases[1].
36 Numerous clinical studies using ginseng extracts have shown that ginseng improves immune
37 functions and cognitive and physical performance and can be used to treat cancer and
38 cardiovascular diseases[1, 2, 3, 4].

39 Ginseng is the collective name for thirteen species in the Panax genus in the Araliaceae
40 family. Among them, *Panax ginseng* (Asian ginseng), *Panax quinquefolius* (American
41 ginseng), and *Panax notoginseng* (sanqi) have been extensively studied for their panacea or
42 "cure-all" medicinal effects[5]. To date, more than 200 chemicals have been identified from *P.*
43 *ginseng*[6, 7, 8]. These include various small-molecule metabolites, such as triterpenes, saponins,
44 polyacetylenes, alkaloids, phenolics, and biopolymers such as polysaccharides, peptidoglycans,
45 and proteins[6, 7, 8]. Currently, ginsenosides, a class of steroidal glycosides and triterpene
46 saponins, are thought to be the principal active compounds in ginseng[1, 3, 9]. Specifically, two
47 major ginsenosides, the protopanaxdiol-type Rb1 and the protopanaxtriol-type Rg1, have been
48 reported to elicit anti-inflammatory and cardioprotective activities, partially through the
49 androgen, estrogen, and glucocorticoid receptors[10, 11, 12, 13]. However, other families of natural
50 products conferring the cure-all or panacea effects of *P. ginseng* remain to be discovered.

51 Peptides are conspicuously absent among ginseng's families of bioactive compounds.
52 A common belief in natural product drug discovery is that peptides are too labile to heat and
53 proteases to have significant therapeutic value, especially when taken orally. However, heavily
54 cross-linked peptides, known as cysteine-rich peptides (CRPs), could be exceptions due to their
55 high tolerance to heat and proteolytic degradation[14, 15, 16, 17]. Recently, we discovered
56 ginsentides, which are glycine- and cysteine-rich peptides with 31–33 amino acids and four
57 disulfide bonds[18]. The disulfide arrangement in ginsentides is different from all known plant

58 CRPs and forms a highly constrained pseudocyclic, with cysteine flanking both the N- and C-
59 termini that form loops with the internal cysteine[18]. As a result, pseudocyclic ginsentides are
60 highly resistant to proteolytic degradation[18]. Representative examples include ginsentide TP1,
61 TP3, and TP8, from *Panax ginseng* and *Panax notoginseng*, *Panax ginseng*, and *Panax*
62 *quinquefolius*, respectively, are all 31 amino acid residues long, highly homologous and found
63 abundantly in ginseng plants (**Fig.1**).

64 The panacea effect of ginseng, as described in ancient texts such as "The Divine
65 Farmer's Materia Medica" and "The Yellow Emperor's Classic of Internal Medicine", includes
66 medicinal benefits like invigorating and restoring cellular homeostasis by revitalizing visceral
67 organs, stimulating rapid recovery from illnesses, improving blood circulation, counteracting
68 the effects of physical and emotional stress, relieving fatigue, and improving stamina[19, 20, 21, 22].
69 Consequently, ginseng is widely prescribed to treat many diseases. An example is the highly
70 influential "Treatise on Febrile Diseases", which documents 113 classic formulations, of which
71 at least 20 contain ginseng[23]. A modern-day interpretation of ginseng's medicinal value is that
72 it is a general tonic for overall health, boosts the immune system, helps prevent illness, and
73 improves overall physical and mental stress adaptation[24, 25, 26, 27]. Because of its ability to
74 modulate the body's stress response and restore balance, ginseng is also an adaptogen[28].
75 However, the current known active compounds based on ginsenosides cannot adequately
76 explain the panacea effects of ginseng.

77 Here, we show that ginsentides, a novel family of bioactive peptides, are adaptogns by
78 eliciting diverse physiological functions that confer cardiovascular benefits, contributing to the
79 anti-stress and panacea effects attributed to ginseng in traditional medicine.

80

81 **Results**

82 **Preparation of ginsentides TP1, TP3, and TP8 from three common ginseng plants**

83 For target identification, validation, and functional studies, we selected the three most
84 abundant ginsentides: TP1, found in *P. ginseng* and *P. notoginseng*, TP3, found in *P. ginseng*
85 and *P. quinquefolius*, and TP8 from *P. quinquefolius*. All three have highly conserved
86 sequences, with TP1 differing from TP3 and TP8 by five and two amino acid residues,
87 respectively. Previously, we showed that the distributions of ginsentides are species and tissue-
88 dependent[18]. We performed large-scale extraction and purification of ginsentide TP1 from *P.*
89 *notoginseng* flowers, TP8 from *P. quinquefolius* flowers, and TP3 from *P. ginseng* seeds. The
90 crude aqueous extracts were fractionated using C18 reversed-phase and strong cation-exchange
91 flash chromatography, and the presence of ginsentides was monitored by mass spectrometry.
92 The concentrated fractions were further purified by reversed-phase high-performance liquid
93 chromatography (RP-HPLC) to achieve a single peak with over 95% purity (**Supplementary**
94 **data S1**). From 1 kg of ginseng flowers or seeds, we obtained approximately 200 mg of
95 ginsentides TP1, TP3, or TP8.
96 In addition to isolating ginsentides from plant materials, we successfully obtained
97 ginsentide TP1 via total chemical synthesis. A synthetic ginsentide precursor was prepared
98 using a stepwise solid-phase synthesis method. After TFA cleavage to remove the protecting
99 groups and release it from the resin support, the S-reduced linear precursor was immediately
100 subjected to oxidative folding under anaerobic conditions, followed by purification using RP-
101 HPLC. The purified synthetic ginsentides, such as ginsentide TP1, were identical to their native
102 form as determined by RP-HPLC, MS, and 1D and 2D NMR. This suggests that these synthetic
103 ginsentides are chemically identical to native ginsentides and that their disulfides are correctly
104 folded (**Supplementary data S2**).
105

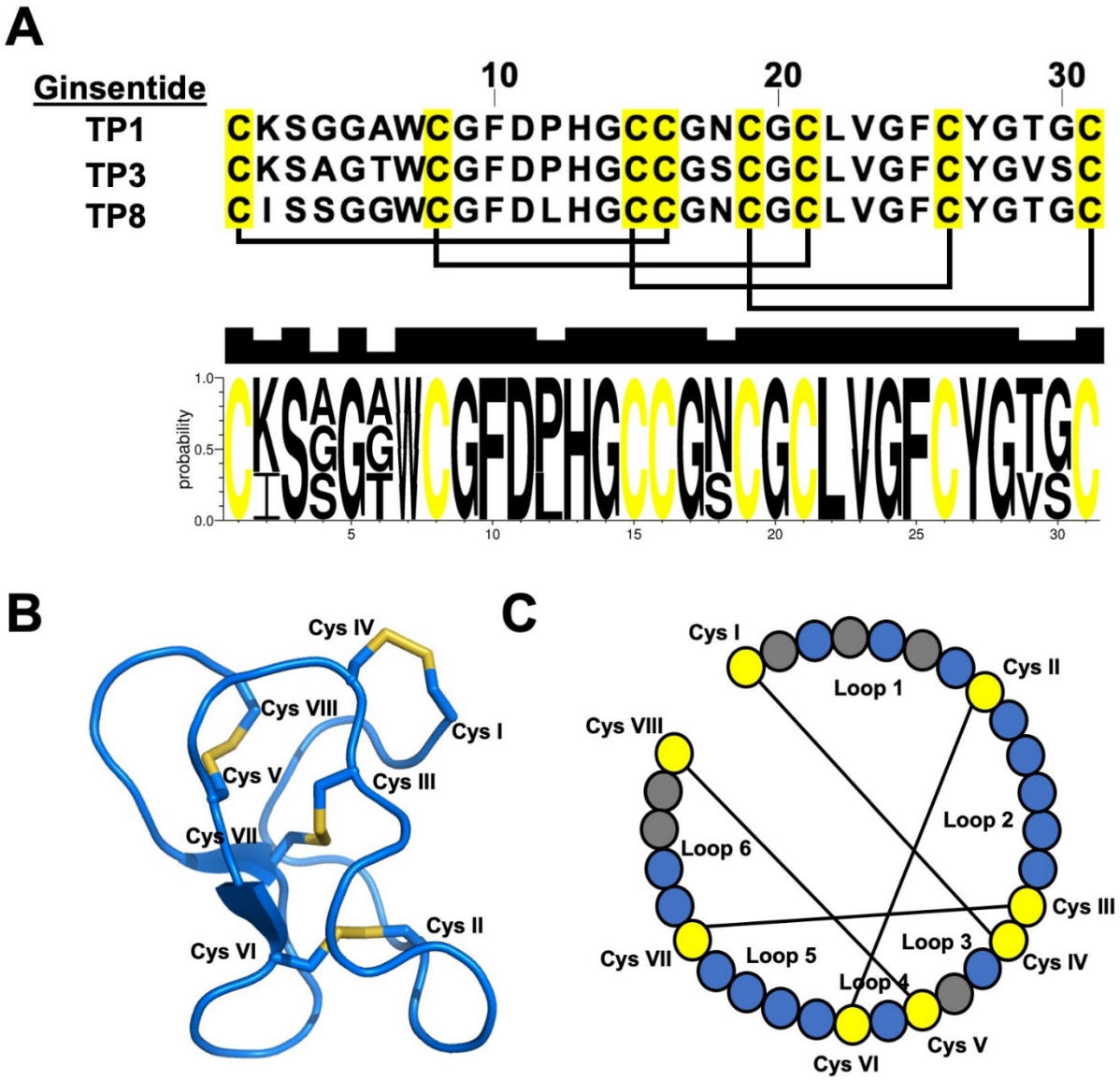

Fig. 1 (A) Primary amino acid sequences of ginsentide TP1 (*Panax ginseng* and *P. notoginseng*), TP3 (*P. ginseng*), and TP8 (*P. quinquefolius*). Web logo showing the highly conserved and homologous amino acid residues of ginsentides TP1, TP3, and TP8. (B) The tertiary structure of ginsentide TP1 (PDB: 2ML7). (C) Illustration of the primary amino acid sequence of TP1, TP3, and TP8, with the colored circles representing amino acid residues (yellow: cysteine; blue: conserved amino acid residues; gray: unconserved amino acid residues) and lines representing disulfide linkages.

115 **Ginsentide TP1 is a cell-penetrating peptide**

116 Our previous studies showed that certain structural-compact and hydrophobic plant-
117 derived cysteine-rich peptides can internalize into cells to interact with intracellular protein
118 targets[17, 29]. To investigate whether the hydrophobic and structural-constrained ginsentides are
119 cell-penetrating, we prepared fluorescent-labeled Cy3-TP1 using cyanine 3 (Cy3)-N-
120 hydroxysuccinimide ester at its lysine sidechain. **Fig. 2A** shows that Cy3-TP1 was internalized
121 into HUVEC-CS cells using confocal microscopy. The cellular uptake of Cy3-TP1 at 4 °C was
122 substantially reduced compared to 37 °C using flow cytometry (**Fig. 2D**). Pre-treating cells
123 with endocytosis inhibitors reduced Cy3-TP1 uptake (**Fig. 2E**). These results suggest that the
124 cellular uptake of Cy3-TP1 involves energy-dependent endocytosis and ginsentide TP1 may
125 have intracellular targets.

126

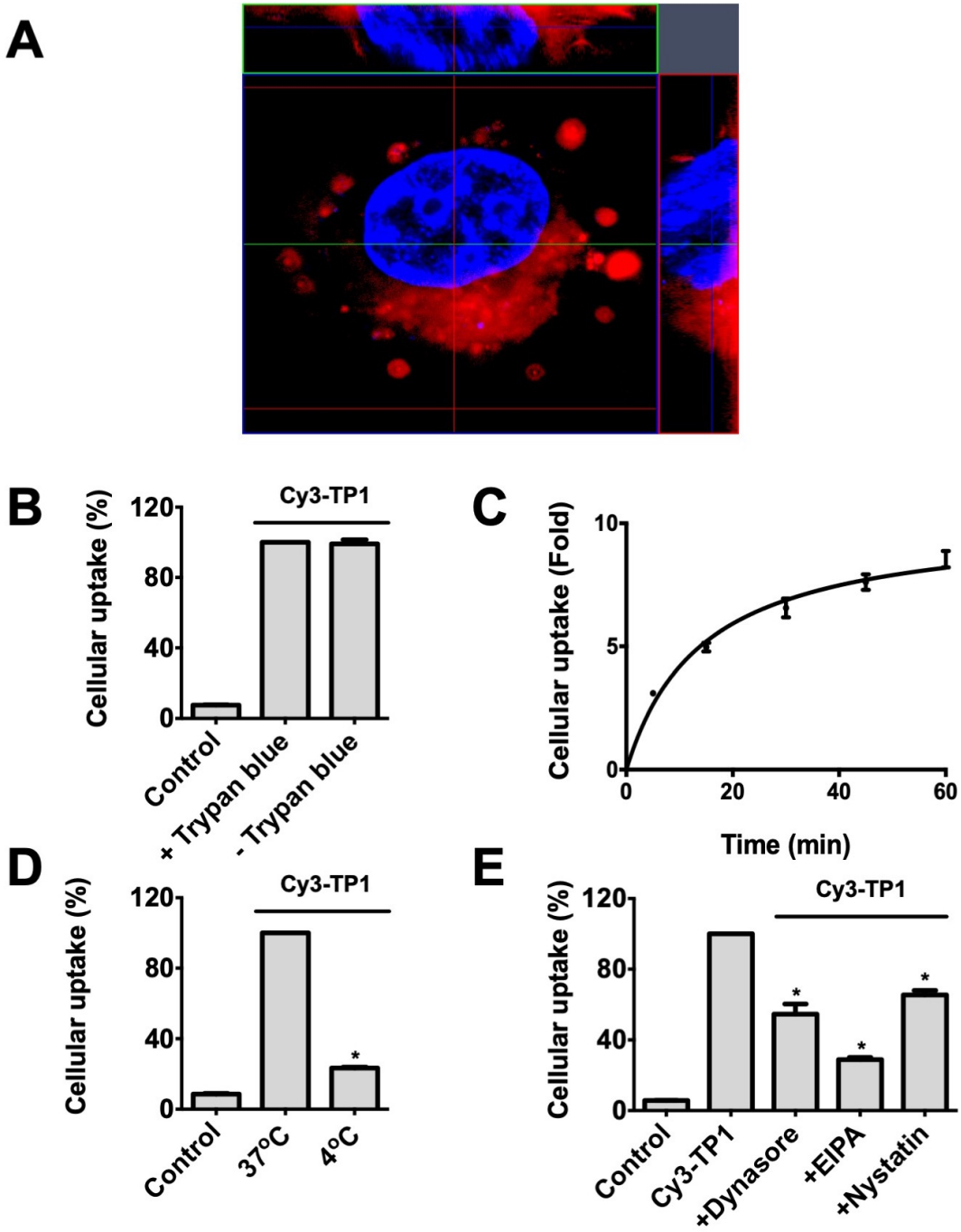

127

128 **Fig. 2 Cy3-TP1 is cell-penetrating.** (A) Z-stack image of Cy3-TP1 in HUVEC-CS cells using

129 confocal microscopy. Using flow cytometry, the cellular uptake of Cy3-TP1 into HUVEC-CS

130 cells was (B) unaffected by trypan blue, (C) time-dependent, (D) temperature dependent, and

131 (E) affected by endocytosis inhibitors (Dynasore, EIPA, and Nystatin). All results are

132 expressed as mean ± S.E.M. from three separate experiments. *$p < 0.05$ compared to control.

133

134 **Proteomic profiling and target identification of intra- and extracellular proteins of**

135 **ginsentide TP1**

136 To identify the intra- and extra-cellular targets of ginsentide TP1, we used affinity-

137 enrichment MS profiling. Again, we immobilized ginsentide TP1 at the lysine sidechain with

138 UltraLink Neutravidin agarose resins for target identification. Three separate experiments were

139 performed, and the samples were tested in triplicate. A pull-down assay followed by LC-

140 MS/MS analysis revealed that 256 proteins were uniquely identified in the ginsentide TP1 pull-

141 down samples (**Figure 3**) (**Dataset 1** and **2**), after removing the background proteins found in

142 parallel control experiments. Bioinformatics analysis of the ginsentide TP1 interactome data

143 suggested the involvement of several important biological pathways, including PIP3 activation,

144 Akt signaling, platelet homeostasis, the MAPK family signaling cascade, interleukin-1

145 signaling, mTORC1-mediate signaling, L1CAM interactions, and cellular stress responses

146 (**Dataset 3**).

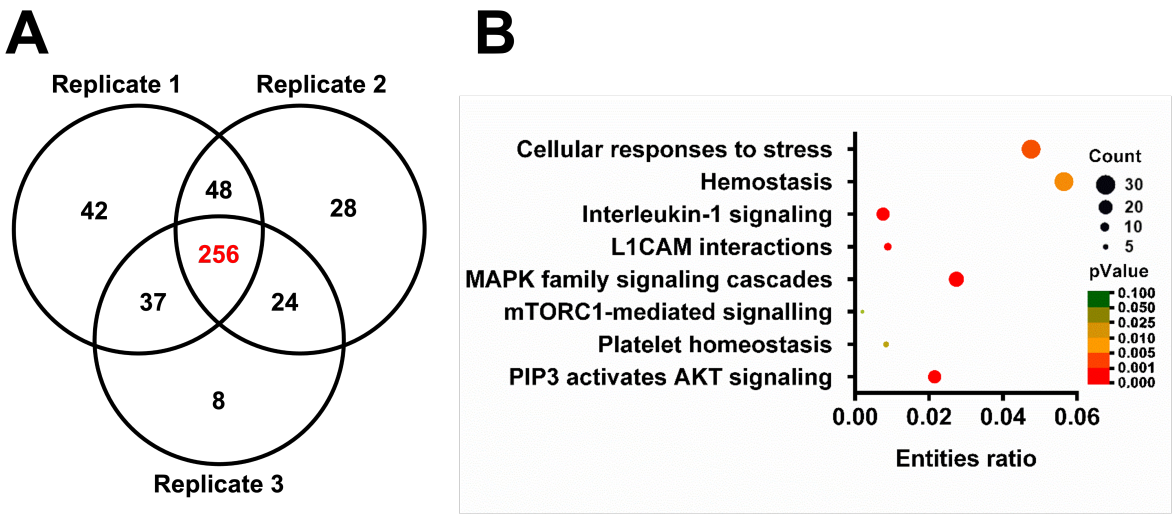

147

148 **Fig. 3 Proteomic profiling of intra- and extra-cellular targets of Ginsentide TP1.** (A) Venn

149 diagram of the uniquely identified proteins for ginsentide TP1 from three experimental

150 replicates. (B) Enriched interacting pathways of ginsentide TP1. Online bioinformatics tool

151 Reactome (https://reactome.org/) was used for the pathway analysis.

152

153 **Ginsentides produce endothelium-derived nitric oxide through PI3K/Akt/eNOS**

154 The cardiovascular effects of ginseng extracts have been extensively studied, and
155 several reports have shown that they have vasodilatory and blood pressure-lowering effects by
156 increasing nitric oxide (NO) levels[30, 31, 32]. NO is a crucial signaling molecule that expands the
157 blood vessels and maintains proper vascular tone. The Akt pathway controls the regulation of
158 NO production[33]. Supported by our proteomic analyses that ginsentide TP1 affects Akt
159 signaling, we examined the effects of ginsentide TP1 on NO production in endothelial cells
160 and its relationship with the Akt signaling pathway. Our results show that ginsentides TP1 (*P.*
161 *ginseng* and *P. notoginseng*), TP3 (*P. ginseng*), and TP8 (*P. quinquefolius*) increase NO
162 production in endothelial cells (**Fig. 4A** and **B**). Ginsentide TP1 was three times more effective
163 than ginsenosides Rb1 and Rg1 on a molar basis (**Fig. 4A**). To eliminate the possibility of
164 ginsenoside contamination in our naturally derived ginsentides, we showed that the synthetic
165 ginsentide TP1 exerts similar effects as its native form (**Fig. 4C**).

166 Activating intracellular eNOS results in NO formation[34]. To confirm that ginsentide
167 TP1-induced NO production depends on NOS activity, we pre-treated endothelial cells with L-
168 N^G-nitroarginine (L-NNA), a competitive inhibitor of NOS. Pre-treatment with L-NNA
169 inhibited ginsentide TP1-induced NO production. In support, Western blot analysis showed
170 that ginsentide TP1 induced phosphorylated eNOS (p-eNOS) accumulation in a concentration
171 and time-dependent manner (**Figs. 4E–G**). The PI3K-Akt pathway can activate eNOS for NO
172 formation[35]. To demonstrate the involvement of ginsentide TP1 in the PI3K-Akt pathway, we
173 pre-treated endothelial cells with an Akt inhibitor, MK 2206, or a PI3K inhibitor, LY294002.
174 Our results showed that both inhibitors decreased ginsentide TP1-induced NO production
175 (**Supplementary data S3A** and **B**). Western blot analysis also showed that ginsentide TP1

176 induced Akt phosphorylation in a time-dependent manner (**Supplementary data S3C**). These

177 results support that ginsentides elicit endothelial NO production through the PI3K-Akt pathway.

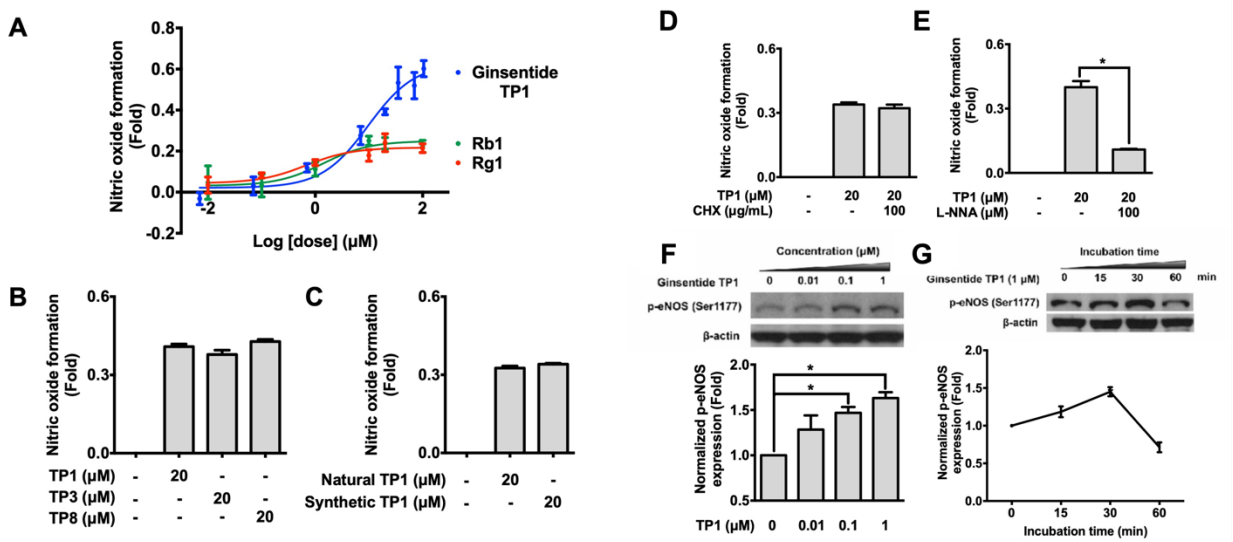

178

179 **Fig. 4 Ginsentides promote nitric oxide (NO) formation from endothelial cells.** (A)

180 HUVEC-CS cells were exposed to ginsentide TP1 and ginsenosides Rg1 and Rb1 for 1 h. (B)

181 HUVEC-CS cells were exposed to ginsentides TP1, TP3, and TP8 for 1 h. (C) HUVEC-CS

182 cells were exposed to natural and synthetic ginsentide TP1 for 1 h. (D) HUVEC-CS cells were

183 exposed to ginsentide TP1 with and without cycloheximide treatment, a protein translation

184 inhibitor, or (E) L-N^G-Nitroarginine (L-NNA), a competitive inhibitor of nitric oxide (NO)

185 synthase for 1 h. Intracellular NO formation was measured with DAF-2 DA staining and

186 expressed as normalized fluorescence intensity. Representative western blot analysis on the (F)

187 dose-dependent effects and (G) time-dependent effects of ginsentide TP1 on phosphorylated

188 eNOS (p-eNOS) accumulations in HUVEC-CS cells. All results are expressed as mean ±

189 S.E.M. in three separate experiments. *$p < 0.05$ compared to the control.

190

191

192 **Ginsentides reduce phenylephrine-induced vasoconstriction**

193 Stress affects catecholamine release, leading to sympathetic overactivity[36, 37].
194 Phenylephrine, a catecholamine similar to adrenaline and a selective α1-adrenergic receptor
195 agonist, was used to induce sympathetic nervous system activation, resulting in blood vessel
196 constriction and increased arterial blood flow. To demonstrate that ginsentides restore the
197 impaired homeostasis associated with sympathetic overactivity, we used isolated rat aortic
198 rings in an ex vivo model to determine their vascular responses[38]. The aortic ring was pre-
199 contracted with either phenylephrine or KCl. Isometric tension measurements showed that
200 ginsentides TP1, TP3, and TP8, and synthetic TP1 reduced phenylephrine-induced but not
201 KCl-induced aortic ring contractions (**Fig. 5**). The EC_{50} of TP1, TP3, and TP8 was
202 approximately 0.1 μM (**Fig. 5A–C**). In contrast, ginsenosides Rb1 and Rg1 did not induce
203 vasorelaxation when tested at concentrations up to 1 μM (**Fig. 5D and E**). Ginsentides TP1,
204 TP3, and TP8 were selective for the α1-adrenergic receptor because they did not elicit
205 relaxation of acetylcholine-induced bladder smooth muscle contraction and did not affect
206 sodium and potassium ion channel activity when tested at concentrations of up to 5 μM
207 (**Supplementary data S4-S8**). These data support that ginsentides alleviate the vascular
208 function of α1-adrenergic receptor overactivity.

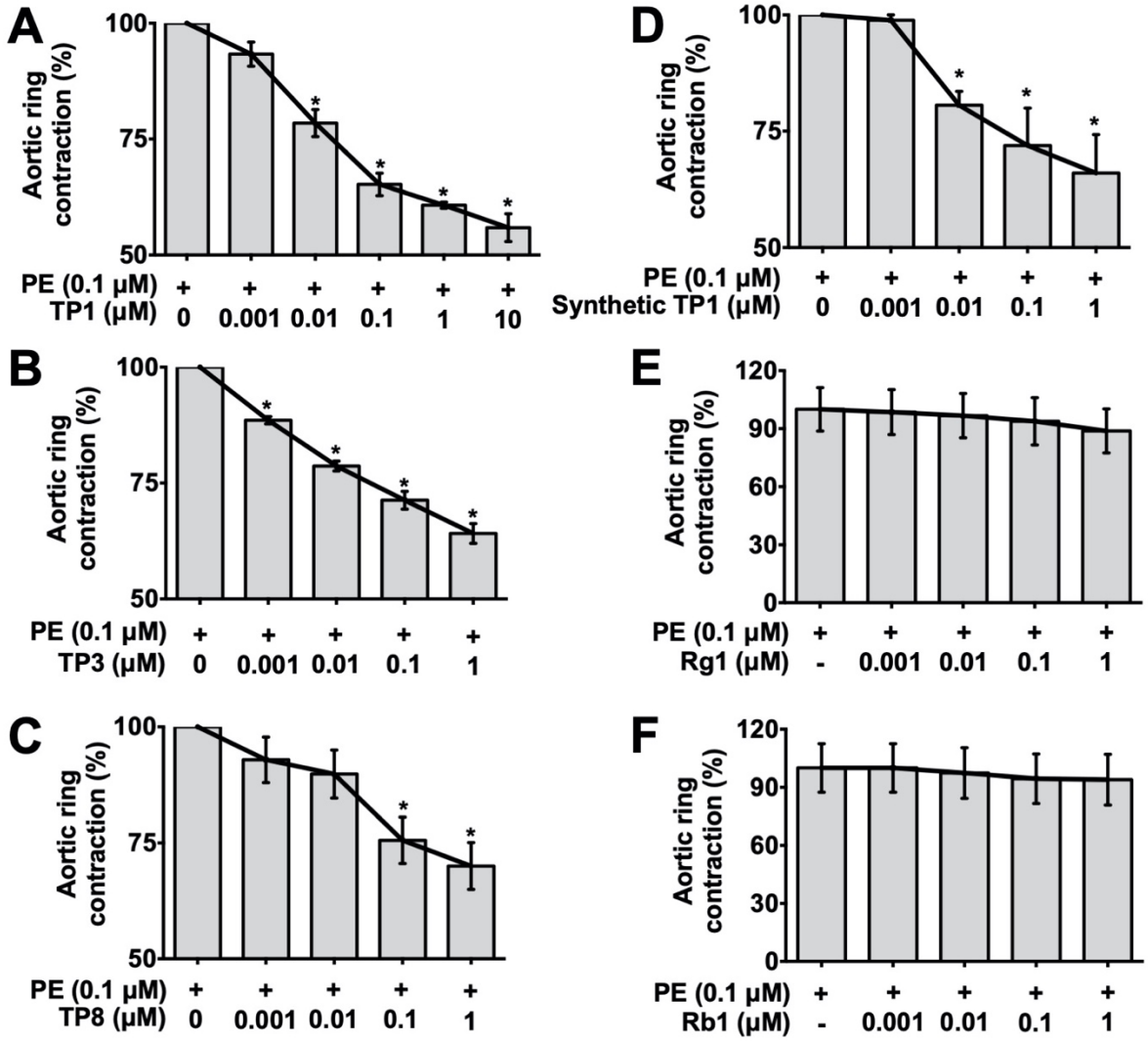

Fig. 5 Ginsentides reduced phenylephrine-induced rat aortic ring contractions. The vascular responses of ginsentides were studied using phenylephrine (0.1 μM) pre-contracted aortic rings in isolated organ chambers. **(A)** TP1 (*P. ginseng* and *P. notoginseng*), **(B)** synthetic TP1, **(C)** TP3 (*P. ginseng*), **(D)** TP8 (*P. quinquefolius*), **(E)** ginsenoside Rg1, and **(F)** ginsenoside Rb1. The responses (isometric tension) were measured with a force-displacement transducer. Aortic ring contractions were measured in volts and are expressed as a percentage compared to controls. All results are expressed as mean ± S.E.M. from three separate experiments. *$p < 0.05$ compared to the control.

219 **Ginsentides reduce monocyte adhesion to endothelial cells**

220 Extended periods of stress can lead to chronic inflammation, contributing to the
221 development of cardiovascular diseases such as atherosclerosis[39, 40, 41]. One of the earliest
222 cellular events in the development of these lesions is the adherence of cells to the endothelium[40,
223 41]. *P. notoginseng* is commonly used to treat cardiovascular diseases related to atherogenesis[42].
224 Studies have shown that ginsenosides Rg1 and Rb1 have potential anti-atherogenic effects[43,
225 44]. Using affinity-enrichment MS, we identified CD166 (ALCAM), CD40, and ESAM as
226 putative targets involved in mediating cell adhesion. To support these findings, we performed
227 pull-down assays and confirmed that ginsentide TP1 interacts with CD166 (ALCAM), CD40,
228 and ESAM (**Fig. 6A-C**).

229 To show that ginsentide TP1 can interfere with cell adhesion, we co-incubated
230 ginsentide TP1 with fluorescent-labeled THP-1 monocytic cells and loaded them onto an
231 endothelial monolayer. Ginsentide TP1 dose-dependently inhibited the basal adhesion of
232 fluorescent-labeled THP-1 monocytic cells to the endothelial monolayer. This was compared
233 with ginsenosides Rg1 and Rb1, which showed weaker inhibitory effects (**Fig. 6D**). The
234 inhibitory effects of ginsentide TP1 were five times more potent than the known adhesion
235 inhibitory peptides (GRGDSP, positive control).

236

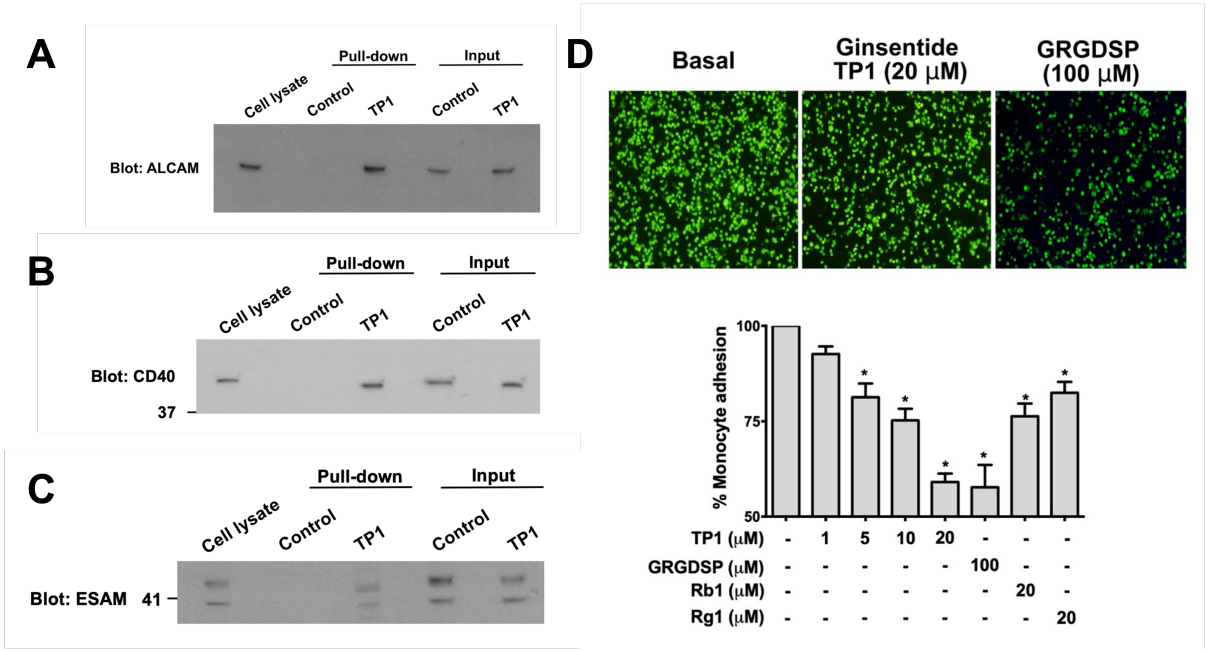

Fig. 6 Ginsentide TP1 reduce monocyte adhesion by interacting with adhesion molecules. **(A)** Ginsentide TP1 interacts with CD166 as revealed by the pull-down western blot analyses using anti-CD166 mAb. **(B)** Ginsentide TP1 interacts with CD40 as the pull-down western blot analyses using anti-CD40 mAb. **(C)** Ginsentide TP1 interacts with ESAM as revealed by the pull-down western blot analyses using anti-ESAM mAb. **(D)** Ginsentide TP1 reduces monocyte adhesion to endothelial cells. Ginsentides TP1 and ginsenosides Rg1 and Rb1 were pre-incubated with HUVEC-CS cells for 30 min and then co-incubated with CFSE-labeled THP-1 monocytic cells for 1 h. Monocyte adhesion was measured by the fluorescence intensity of CFSE. All results are expressed as mean ± S.E.M. from three separate experiments. *$p < 0.05$ compared to the control.

Ginsentides reduce platelet aggregation and thrombus formation

Chronic stress can activate the sympathetic nervous system, leading to the continual release of stress hormones, which may result in excessive blood clotting[36, 39]. Conditions such as atherosclerosis, deep vein thrombosis, and pulmonary embolism may occur[36, 39]. Ginseng reduces thrombotic events and improves cardiovascular health through antiplatelet

254 mechanisms[4, 45, 46, 47]. Results from affinity-enrichment MS suggest that ginsentide TP1 affects
255 platelet homeostasis. Additionally, ginsentide TP1 was an antagonist for the P2Y12 receptor
256 when tested against a panel of 168 GPCR targets. **Fig. 7A** shows the dose-response curve of
257 ginsentide TP1 inhibiting P2Y12, with an IC50 of approximately 20 μM. Conversely,
258 ginsenosides Rb1 and Rg1 did not display inhibitory effects against P2Y12 activation at similar
259 concentrations (**Figs. 7B and C**).

260 Using an *ex vivo* platelet aggregation model, we determined the effects of ginsentide
261 TP1 after intravenous or oral administration. Our results showed that ginsentide TP1 reduced
262 platelet aggregation in response to ADP stimulation (**Fig. 7D** and **E**). These results also indicate
263 that ginsentide TP1 is orally active.

264 We tested the anti-thrombotic effects of ginsentide TP1 *in vivo* in an acute thrombotic
265 mouse model[48]. Acute pulmonary thrombosis was induced by tail vein injection using a
266 combination of collagen and adrenaline[48]. Oral pre-treatment with ginsentide TP1 (10 mg/kg
267 and 30 mg/kg) for three consecutive days significantly reduced thrombus formation in the lung
268 compared to the saline control group. These effects were comparable to oral administration
269 with the positive controls, clopidogrel (50 mg/kg) or aspirin (100 mg/kg) (**Fig. 7F**).

270

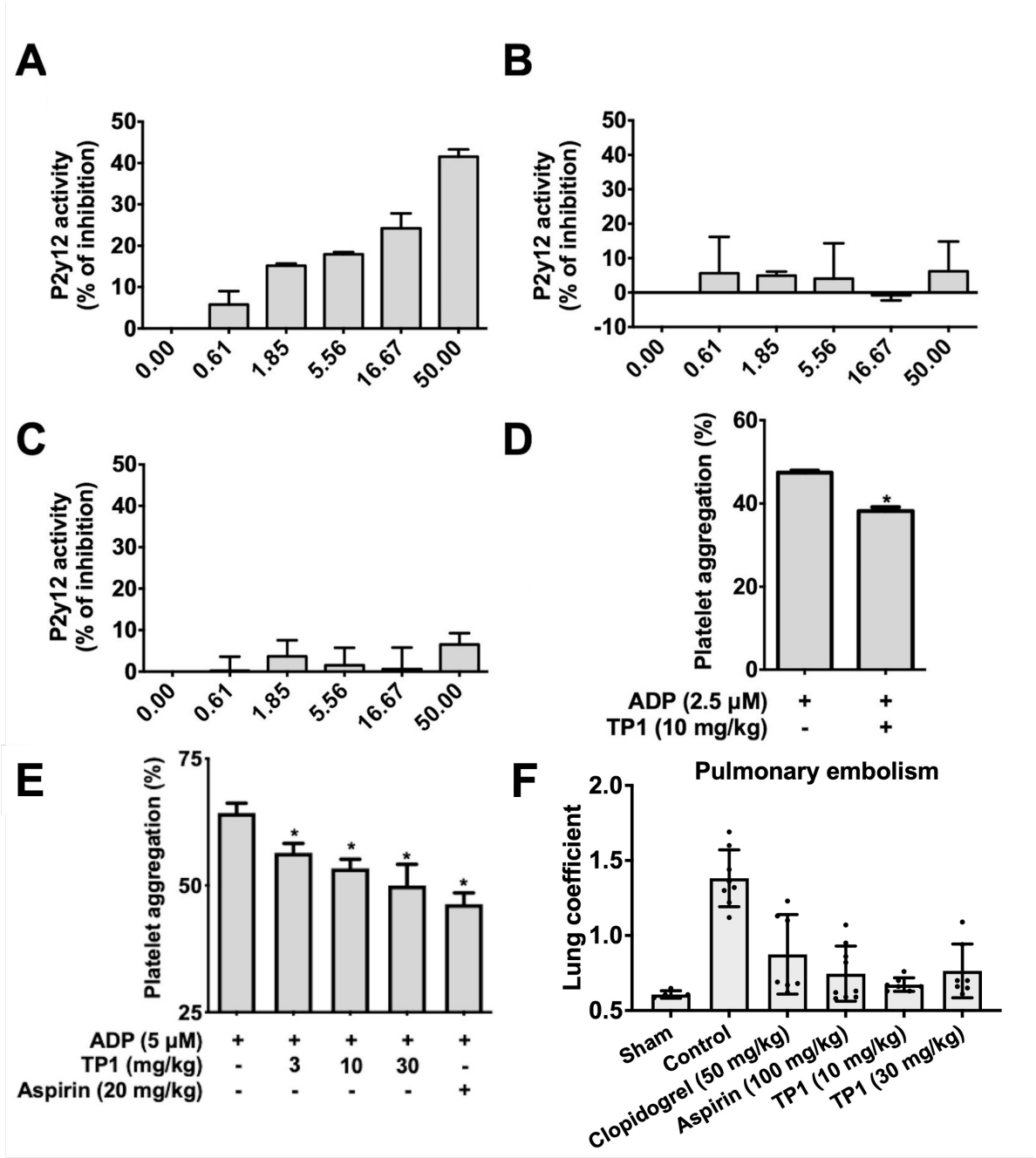

Fig. 7 Ginsentides reduce platelet aggregation *ex vivo*. Ginsentide TP1, but not ginsenosides Rg1 and Rb1, inhibits P2Y12 activation. Effects of **(A)** ginsentide TP1, **(B)** ginsenoside Rg1, and **(C)** ginsenoside Rb1 on P2Y12 activation were analyzed with the Pathhunter eXpress β-arrestin kit (N = 2). Ginsentide TP1 (10 mg/kg) or PBS was **(D)** Intravenous injection of ginsentide TP1 (10 mg/kg) or PBS or **(E)** oral gavage of ginsentide TP1 (3, 10, 30 mg/kg) or PBS to SD rats were conducted once daily for 3 days. 30 min after the final pre-treatment, blood samples were collected, and platelets were concentrated by centrifugation. Platelet

279 aggregation was initiated by ADP. The percentage of platelet aggregation was determined by
280 optical density (N = 5; *p < 0.05). **(F)** Effects of oral-administered ginsentide TP1 on collagen
281 plus adrenaline-induced acute lung thrombosis in mice.
282
283 **Behavioral Tests: Tail suspension and forced swimming**
284 Based on our experimental data, ginsentides may modulate the "fight-or-flight"
285 response, a physiological stress response. Clinically, chronic stress can lead to depression-like
286 behavioral changes[49, 50]. Using two well-established behavioral assays, forced swimming and
287 tail suspension[51, 52], we assessed the effects of ginsentide TP1 on responses to depressive-like
288 behavior in mice. Both experiments are based on measuring the duration of immobility when
289 the mice are exposed to an inescapable situation[51, 52]. To determine the potential antidepressant
290 activity of ginsentide TP1, we assessed the immobility time after oral administration to mice.
291 The forced swimming test showed that ginsentide TP1 (30 mg/kg) and the fluoxetine (20
292 mg/kg), positive control significantly decreased the immobility time by 71.68 ± 9.963 s and
293 42.52 ± 9.963 s, respectively (**Fig. 8**). Similarly, in the tail suspension test, ginsentide TP1 (30
294 mg/kg) and fluoxetine (20 mg/kg) as a positive control significantly decreased the immobility
295 time by 41.38 ± 7.054 s and 30.01 ± 7.219 s, respectively (**Fig. 9**). Together, these studies
296 suggest that ginsentide TP1 has anti-stress effects.
297

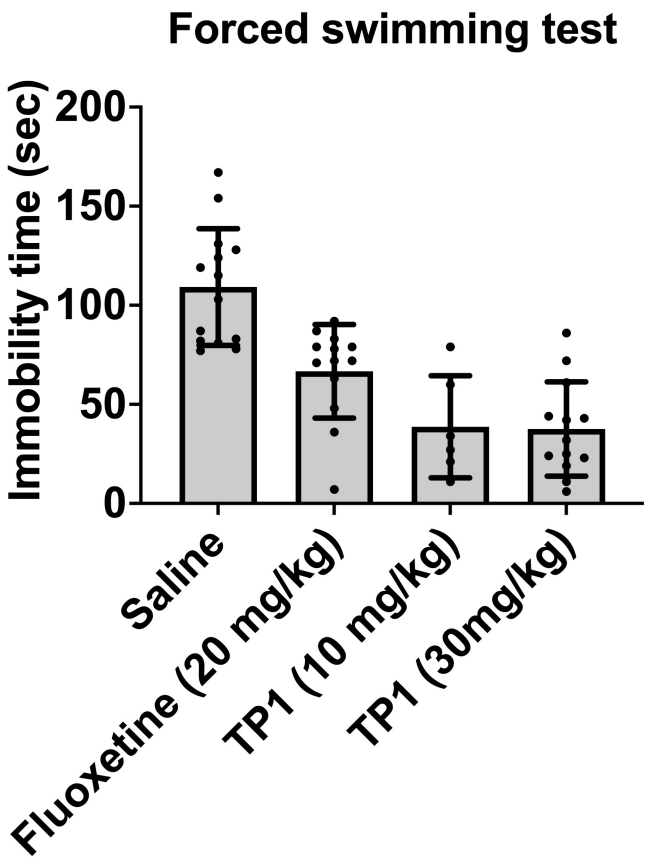

Fig. 8 Behavioral performance of mice in the forced swimming test. Immobility period of mice in the swimming endurance stress assay measured after treatment with fluoxetine (20 mg/kg) (positive control) or different concentrations (10 or 30 mg/kg) of TP1.

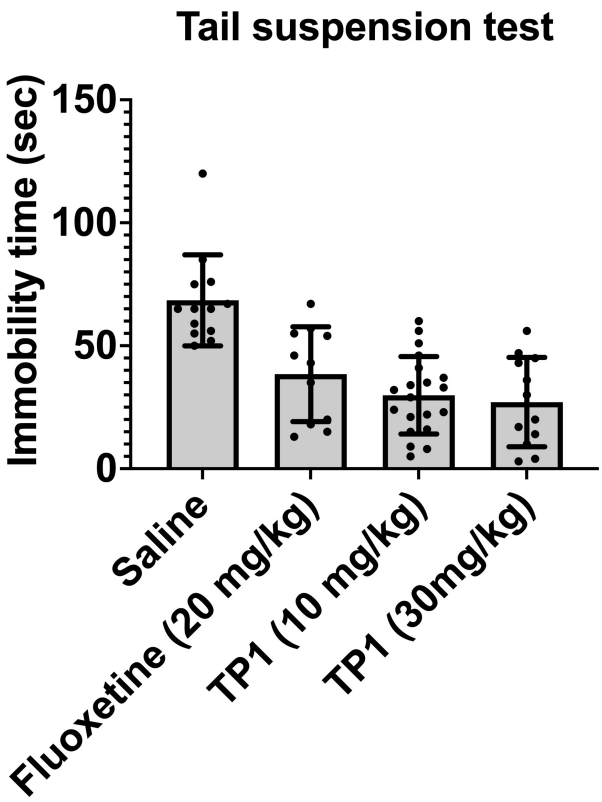

Fig. 9 Behavioral performance of mice in the tail suspension test. Immobility period of mice in the tail suspension stress assay after oral treatment with fluoxetine (20 mg/kg) (positive control) or different concentrations (10 or 30 mg/kg) of TP1.

Discussion

Stress is a multifaceted response to a perceived threat involving physiological and psychological changes[54]. Physiologically, the body manages stress through the "fight-or-flight" response, activating the sympathetic nervous system and releasing stress hormones like adrenaline and cortisol[55, 56]. These hormones then stimulate natural physiological reactions, including an increase in heart rate and blood pressure and activation of the coagulation cascade[56]. However, in situations such as chronic stress, erratic counteracting mechanisms may arise, resulting in physical and psychological disorders like cardiovascular diseases and depressive-like behavior[36, 39, 49, 54]. In this report, we used a combination of methods, *in vitro*-, *ex vivo*-, and *in vivo*-studies to demonstrate that ginsentides TP1, TP3, and TP8 are novel

318 bioactive peptides and could represent major contributors to the adaptogenic effects of ginseng
319 in relieving stress-related disorders.

320 To counter stress, the body uses various physiological systems, including the activation
321 of various cardiovascular functions via multiple mechanisms[56]. *P. ginseng*, *P. quinquefolius*,
322 and *P. notoginseng* are frequently prescribed in traditional medicine to promote blood
323 circulation, earning them a high reputation for their cardiovascular benefits[4, 24, 44]. Specifically,
324 we show that ginsentides increase NO production in endothelial cells, promote vasorelaxation,
325 reduce cell adhesion and platelet aggregation, and improve depressive-like behaviors.
326 Currently, ginsenosides are considered the major active compounds in ginseng. However, they
327 do not fully explain the adaptogenic effects elicited by a whole-ginseng mixture.

328 Ginseng is generally regarded as safe for food supplements and traditional medicinal
329 uses[25, 53]. Guided by traditional medicines, we have conducted a decade-long research program
330 to identify orally-active super cystine-dense peptides or microproteins from medicinal plants.
331 These microproteins, with 6-10 cysteine residues and a molecular weight of 2-4 kDa, are
332 bioactive and show potential as therapeutic leads for cardiovascular diseases, stress, frailty, and
333 other chronic and age-related diseases. Previously, we identified ginsentides as a group of
334 plant-derived peptides or microproteins found in different ginseng species[18]. Currently, 14
335 different ginsentides have been identified. They are cystine-dense (>24% cysteine), highly
336 homologous, 31–33 amino acids in length, with eight cysteine residues forming a unique
337 disulfide connection[18]. Consistently, we previously showed that TP1 is non-toxic in Huh7 cells
338 or red blood cells at concentrations up to 100 μM[18], a concentration at least 5-fold higher than
339 the dosages used in this paper. Furthermore, we showed that TP1 is non-immunogenic to THP-
340 1 cells, with no observable increase in IL-6, IL-8, IL-10, and TNFα[18].

341 Ginsentides TP1, TP3, and TP8 from *P. ginseng* and *P. notoginseng*, *P. ginseng*, and
342 *P. quinquefolius*, respectively, share ~85% homology in their primary sequences in which the

343 eight cysteine residues, and cystiene motif are absolutely conserved. They are proteinaceous
344 natural products. Interestingly, we found that ginsentides and ginsenosides which are small-
345 molecule metabolites share similarity in certain bioactive functions but differ in magnitude.
346 For example, ginsentide TP1 is more effective than ginsenosides in promoting NO production,
347 reversing the vasoconstriction caused by phenylephrine, and reducing cell adhesion. Using
348 GPCR profiling, we found that ginsentide TP1 can inhibit ADP-induced P2Y12 receptor
349 activation, which could lead to reduced platelet aggregation *ex vivo* and thrombus formation *in*
350 *vivo*. However, ginsenosides Rb1 and Rg1 show no activity against ADP-induced P2Y12
351 activation. Thus, ginsentides TP1, TP3, and TP8, represent not only the "first-in-class" active
352 compounds in ginseng, but also a missing link in the "cure-all" use of ginseng in traditional
353 medicines.

354 The identification of ginsentides as bioactive and proteolytic-stable peptides underscore
355 the emergence of constrained peptides as active compounds in herbal medicines. Ginsentides,
356 similar to other cysteine-rich peptides, including roseltides, bleogens, chenotides, and
357 avenatides[14, 15, 57, 58], are structurally constrained by multiple disulfides to render them resistant
358 to proteolytic degradation, making them potentially orally active[14, 15, 16, 17, 29]. Because
359 ginsentides have a cystine-dense core, they have an "inside-out" conformation, causing the side
360 chain of hydrophobic amino acids to be exposed[17, 29]. These exposed hydrophobic patches
361 found in ginsentides as well as many CRPs such as roseltides from *Hibiscus sabdariffa*[17, 29],
362 can drive cell-penetration, allowing their internalization into cells to target intracellular
363 targets[16, 17, 29, 57, 58]. The ability of ginsentides to target both extracellular and intracellular
364 protein targets represent a distinctive new feature to this family of natural products.

365

366 **Conclusions**

367 In conclusion, we demonstrated that ginsentides are orally bioactive and play a wide
368 array of functions that provide the adaptogenic and panacea effects of ginseng, particularly for
369 cardiovascular health. Our work greatly expands the known bioactive phytochemicals of
370 ginseng from small molecule metabolites to non-metabolites, peptides, and microproteins and
371 opens new avenues for ginseng research.
372
373 **Methods & Protocol**
374 **Materials**
375 All chemicals and solvents, unless otherwise stated, were purchased from Sigma–
376 Aldrich (St. Louis, MO, United States) and Fisher Scientific (Waltham, MA, United States).
377
378 **Isolation and purification of ginsentides**
379 Ginsentide TP1, TP3 or TP8 were extracted from the dried flowers or seeds of *Panax*
380 ginseng, *Panax quinquefolius,*and *Panax notoginseng* as previously described[18]. Briefly, the
381 plant materials were pulverized and extracted with water. The extracts were filtered and
382 subjected to flash chromatography using C18 powder (Grace Davison). 60% ethanol was used
383 to elute the ginsentide-enriched fractions which were then loaded onto an SP Sepharose resin
384 column (GE Healthcare, UK) and eluted with 1 M NaCl (pH 3.0). Further purification was
385 done using preparative RP-HPLC (Shimadzu, Japan) with a C18 Grace Vydac column (250 ×
386 22 mm) at a flow rate of 8 mL/min, linear gradient of 1%/min of 10–80% buffer B. Buffer A
387 contained 0.05% (v/v) trifluoroacetic acid (TFA) in HPLC grade water, and buffer B contained
388 0.05% (v/v) TFA and 99.5% (v/v) acetonitrile (ACN). Resulting fractions were further purified
389 using a semi-preparative C18 Vydac column (250 × 10 mm) at a flow rate of 3 mL/min with
390 the same linear gradient. The identity of the ginsentide containing fractions were confirmed by

391 matrix-assisted laser desorption/ionization- time of flight mass spectrometry (MALDI-TOF
392 MS; AB SCIEX 5800 MALDI-TOF/TOF).
393
394 **Solid-phase peptide synthesis and oxidative folding**
395 Synthetic ginsentide TP1 was synthesized by Fmoc-based solid-phase peptide synthesis
396 on 2-Chlorotrityl chloride resin as previously described[16]. The linear precursor peptide was
397 cleaved using a cocktail consisting of 92.5 % TFA, 2.5 % H_2O, 2.5 % 1,2-ethanedithiol, and
398 2.5 % triisopropylsilane at room temperature for 30 min followed by precipitation with diethyl
399 ether. The crude cleavage product was folded in 10% dimethyl sulfoxide (DMSO), 90% 0.1 M
400 NH_4HCO_3 (pH 8), cystamine (10 equivalents), and cysteamine (100 equivalents) for overnight
401 at 4 °C. Folded ginsentide TP1 was purified by preparative HPLC (250 x 21 mm, 5 µm;
402 Phenomenex, USA). A linear gradient of mobile phase A (0.1 % TFA in H2O) and mobile
403 phase B (0.1 % TFA in ACN) was used. The folded ginsentide TP1was identified using
404 MALDI-TOF MS. The folding yield was approximately 30%. RP-HPLC and 2-dimensional-
405 nuclear magnetic resonance (2D NMR) were performed to compare the physical properties of
406 synthetic ginsentide TP1 to its native form (**Supplementary data S1 and S2**).
407
408 **Fluorescent labeling of ginsentide TP1**
409 The lysine sidechain of native ginsentide TP1 was fluorescent-labeled using Cy3 NHS
410 ester (Lumiprobe, USA) in 100 mM phosphate buffer (pH 7.8). Fluorescent labeling was
411 carried out at room temperature for 16 h, and Cy3-TP1 was then identified and purified by RP-
412 HPLC and MALDI-TOF MS.
413
414 **Immobilization of ginsentide TP1 onto agarose beads**

415 Ginsentide TP1 was immobilized onto agarose beads using AminoLink™
416 Immobilization Kit (Thermo Fisher Scientific, USA) according to manufacturer instructions.
417
418 **Confocal microscopy analysis**
419 Live-cell confocal microscopy was conducted on HUVEC-CS (human umbilical vein
420 endothelial) cells. HUVEC-CS were cultured in high glucose DMEM containing 1 mM sodium
421 pyurvate, 4 mM L-glutamine supplemented with 10% fetal bovine serum (FBS) and 100 U/mL
422 of penicillin and streptomycin in a 5% CO2 humidified incubator at 37 °C. To examine the
423 intracellular distribution of Cy3-TP1, HUVEC-CS cells were seeded on an 8-well chamber
424 slide (Ibidi, Germany). After incubation with Cy3-rT1, cells were stained with Hoechst 333241.
425 The slides were imaged using a Zeiss LSM 710 confocal microscope.
426
427 **Cellular uptake analyses by flow cytometry**
428 Cellular uptake of Cy3-TP1 was analyzed using flow cytometry, HUVEC-CS cells
429 were incubated with Cy3-TP1 in serum-free medium at 37 °C. Following incubation, cells were
430 harvested and collected by centrifugation at 500 g for 5 min. To quench extra-cellular
431 fluorescence, cells were mixed with 150 μg/mL of trypan blue, and the samples were analyzed
432 by flow cytometry. A total of 10,000 cells were analyzed using a BD LSR FortessaTM X-20
433 flow cytometer. For temperature-dependent uptake studies, HUVEC-CS cells were incubated
434 at 4 °C for 30 min prior to incubation with Cy3-TP1 for 1 h at 4 °C. For endocytosis inhibitor
435 studies, HUVEC-CS cells were pretreated with endocytosis inhibitors, including 50 μM
436 dynasore, 50 μM ethylisopropylamiloride (EIPA), and 50 μg/mL nystatin for 30 min, followed
437 by incubation with Cy3-TP1 for 1 h at 37 °C.
438
439 **Sample preparation and LC-MS/MS analysis**

440 Affinity-enrichment mass spectrometry profiling was performed using immobilized
441 ginsentide TP1 on agarose beads. After washing the beads with phosphate-buffered saline (PBS)
442 three times, 600 μg of HUVEC-CS cell lysate was added to each tube and allowed to incubate
443 overnight at 4 °C with gentle end-to-end rotation. After incubation, the resin was transferred
444 to Pierce®spin columns and washed with PBS. 6X loading dye with 2-mercaptoethanol was
445 added to the resin and heated for 10 min at 85 °C. The resultant mixture was centrifuged at 200
446 g for 1 min and resolved by electrophoresis at 100 V for 120 min using 15% SDS-PAGE. After
447 the samples were resolved on the SDS-polyacrylamide gel, each sample lane was cut. The gel
448 pieces were reduced with 10 mM DTT for 30 min at 60 °C and alkylated for 45 min with 55
449 mM iodoacetamide at room temperature. The samples were then subjected to in-gel tryptic
450 digestion (Promega, USA) at 37 °C overnight. Tryptic peptides were extracted with 5% acetic
451 acid in 50% ACN buffer and vacuum dried.
452 Tryptic peptides were then subjected to LC-MS/MS analysis using a Q Exactive mass
453 spectrometer coupled with an online Dionex Ultimate 3000 RSLC nano-LC system (Thermo
454 Fisher Scientific). Dried tryptic peptides were reconstructed in 0.1% formic acid solution and
455 resolved using a Dionex EASY-spray column (PepMap C18; 3 μm; 100 Å) and injected
456 through an EASY nanospray source. Data acquisition was performed using Xcaliber 2.2
457 (Thermo Scientific). Samples from experimental triplicate were run as technical duplicates.
458 Mascot generic format files were generated from the raw data using Proteome Discoverer
459 1.4.1.14 software). In-house Mascot search engine (version 2.4.1; Matrix Science, UK) was
460 used for the protein sequence database searches The UniProt Knowledgebase of human
461 proteins (downloaded on Feb 19, 2016, including 140450 sequences and 47482854 residues)
462 was used as a search database. Carbamidomethyl at cysteine was set as a static modification
463 and methionine oxidation, asparagine and glutamine deamidation were used as dynamic
464 modifications. Full trypsin digestion with maximum 2 missed cleavages was set as the

465 digestion parameter. The peptide mass tolerance of ± 10 ppm (# ^{13}C = 2) and a ± 0.02-Da for-
466 fragment mass were set as mass tolerance parameters. The data with the significance threshold
467 value of $p<0.05$ and "IgnoreIonsScoreBelow" value of 20 were extracted in *csv format. The
468 False discovery rate (FDR) were calculated using target-decoy search strategy with cutoff set
469 to ≤ 1%and proteins identified with multiple peptides were selected for the final analysis.
470 Proteins identified in all three experimental replicates were only consider for final analysis.
471 Online bioinformatics tool Reactome (https://reactome.org/) was used for the pathway analysis.
472

473 **Nitric oxide measurement**

474 A specific fluorescence probe, 4, 5-diaminofluorescein diacetate (DAF-2 DA), was
475 used to measure cellular NO. HUVEC-CS cells were seeded at a density of 1.0 x 105 cells/mL
476 in a 96-well plate. Cells were first washed with Hank's balanced salt solution (HBSS) prior to
477 treatment with different concentrations of ginsentide TP1 (final DMSO concentration 0.1%)
478 and 5 μM DAF-2 DA. To study the mechanisms involved, cells were pre-incubated with
479 different inhibitors for 1 h followed by another 1 h treatment with ginsentide TP1. Treated cells
480 were incubated for 1 h in the dark at 37 °C. Fluorescence intensity was measured at excitation
481 wavelength 485 nm and emission wavelength 515 nm on an Infinite® 200 PRO series
482 microplate reader. The results were presented as changes in normalized fluorescence intensity
483 compared to control.
484

485 **Western blot analysis**

486 HUVEC-CS cells treated with ginsentide TP1 were harvested with a scraper and lysed
487 in CelLytic™ M lysis buffer supplemented with protease inhibitor cocktail and phosphatase
488 inhibitor cocktail on ice with frequent agitation for 30 min. The cell homogenates were
489 centrifuged at 12000 rpm for 30 min at 4 °C and supernatants were collected. Protein

490 concentrations were determined using bicinchoninic acid (BCA) reagent. Total protein (30 μg)
491 mixed with SDS loading buffer was denatured at 70 °C for 10 min. Denatured protein samples
492 were then electrophoretically resolved on SDS-PAGE and transferred onto a 0.2 μm PVDF
493 membrane. The membranes were blocked for 1 h at room temperature with 5% BSA TBST.
494 The membranes were incubated for 1 h at room temperature or overnight at 4 °C with rabbit
495 primary antibody for total-akt (1:1000) (CAT No. 9272S, Cell Signaling Technology, USA) or
496 rabbit phosphorylated akt (Ser 473) (1:1000) CAT No. 4060S, Cell Signaling Technology,
497 USA) or rabbit phosphorylated eNOS (Ser 1177) (1:1000) (CAT No. 9570S, Cell Signaling
498 Technology, USA) or mouse β-actin (1:10000) (CAT No. A5316, Merck, USA) diluted with
499 5% BSA in TBST. The membrane was then incubated for 1 h at room temperature with
500 horseradish peroxidase-conjugated anti-rabbit (1:2000) (Cell Signaling Technology, USA) or
501 anti-mouse secondary antibody (1:2000) (Cell Signaling Technology, USA) diluted with 5%
502 BSA in TBST. The immune complexes were detected on X-ray film using Advansta
503 chemiluminescent substrate. For re-probing, the membrane was stripped with guanidine
504 hydrochloride stripping buffer (6 M guanidine hydrochloride, 0.2% Nonidet (NP-40), 0.1 M β-
505 mercaptoethanol, 20 mM Tris–HCl, pH 7.5) twice for 5 min, followed by 5 min washing with
506 TBST four times[59]. To determine the intensity of the protein targets, densitometric analysis
507 was performed using NIH Image-J software (National Institutes of Health, USA) and was
508 presented as relative to β-actin expression as an internal control.
509

510 ***Ex vivo* aortic ring contraction**

511 All protocols and procedures were approved by the Animal Care and Welfare
512 Committee of Institute of Materia Medica, Chinese Academy of Medical Sciences and Peking
513 Union Medical College, Beijing, China. Aortic ring contraction studies were performed as
514 previously described with slight modifications[60]. Following decapitation, the thoracic aorta

515 was quickly removed, cleared of fat and connective tissue and cut into segments (rings of
516 approximately 2 mm). Aortic rings were mounted in a 15 mL organ baths containing Krebs
517 buffer (120.4 mM NaCl, 5.9 mM KCl, 2.5 mM $CaCl_2$, 1.2 mM MgCl2, 1.2 mM NaH_2PO_4, 11.5
518 mM glucose, 25 mM NaHCO3, pH 7.5) at 37 °C with continuous 95% O_2 and 5% CO_2 supply.
519 Endothelium-intact aortic rings were pre-constricted with 40 mM KCl, followed by a relaxant
520 response to 30 mM acetylcholine to ensure their integrity and functionality. Aortic rings were
521 then allowed to equilibrate for 40 min prior to isometric tension measurements of vascular
522 contractility. The vascular responses of ginsentide TP1, TP3 and TP8 were characterized in 0.1
523 μM phenylephrine pre-contracted aortic rings. Isometric tension was measured by a force-
524 displacement transducer and recorded using AcqKnowledge ACK100 Version 3.2 (BIOPAC
525 Systems, USA). Aortic ring contractions were measured in volts and expressed as a percentage
526 compared to control.
527
528 **Monocyte–endothelium adhesion assay**
529 Monocyte-endothelium adhesion assay was performed as previously described. Briefly,
530 HUVEC-CS cells were grown until confluent in a 96-black well clear bottom plate. The cells
531 were pre-treated with different concentrations of ginsentide TP1 (1, 5, 10, 20 μM) or 100 μM
532 GRGDSP or 20 μM of ginsenoside Rb1 or 20 μM of ginsenoside Rg1 or PBS for 30 min at 37
533 ºC. After 30 min, HUVEC-CS cells were co-incubated with carboxyfluorescein succinimidyl
534 ester (CFSE)-labeled THP-1 cells at a density of 1×10^6 cells/well in serum-free RPMI medium
535 for 1 h at 37 ºC. Monocyte adhesion was measured by the fluorescence intensity of CFSE after
536 washing five times with PBS using a fluorescence microplate reader.
537
538 **Pull-down assay**

539 Pull-down assays was performed using immobilized ginsentide TP1 on agarose beads.
540 Briefly, immobilized ginsentide TP1 was washed with PBS three times and incubated 600 μg
541 of HUVEC-CS cell lysate was added to each tube and allowed to incubate overnight at 4 °C
542 with gentle end-to-end rotation. After incubation, the mixture was transferred to Pierce®spin
543 columns and washed 10 times with PBS. 6X loading dye with 2-mercaptoethanol was added
544 to the resin and heated for 10 min at 85 °C. The resultant mixture was centrifuged at 200 g for
545 1 min and resolved using 8%-12% SDS-PAGE, at 100 V constant for 120 min. Blot transfer
546 was performed onto a PVDF membrane at 250 mA for 120 min on ice. The blot was blocked
547 with 5% BSA TBST before incubating overnight at 4 °C with anti-CD166 (CAT No. SC-74558,
548 Santa Cruz Biotechnology, USA), or CD40 (CAT No. SC-13128, Santa Cruz Biotechnology,
549 USA) anti-mouse antibody, or anti-ESAM (CAT No. SC-366580, Santa Cruz Biotechnology,
550 USA) anti-rabbit antibody (1:500 in 5% BSA TBST). After incubation overnight, the
551 membrane was washed with TBST at room temperature three times, 10 min each. The blot is
552 then incubated with horseradish peroxidase-conjugated anti-mouse secondary antibody
553 (1:2000) (Cell Signaling Technology, USA) or anti-rabbit (1:2000) (Cell Signaling Technology,
554 USA), diluted with 5% BSA in TBST, for another 1 h at room temperature. The blot was
555 washed five times 10 min each with TBST at room temperature before addition of
556 chemiluminescence substrate and exposure on X-ray film.
557
558 **G-Protein Coupled Receptor profiling**
559 G-Protein Coupled Receptor (GPCR) profiling was conducted using gpcrMAX^{SM}
560 GPCR Assay Panel, a functional cell-based assay, by DiscoverX, USA as a service contract.
561 The effects of ginsentide TP1 on 168 GPCRs were screened in both agonist and antagonist
562 modes.
563

564 **P2Y12 β-Arrestin recruitment assay**

565 P2Y12 β-Arrestin recruitment assay was conducted as previous described by
566 DiscoverX (USA) as a service contract. The effects of ginsentide TP1, ginsenoside Rb1, or
567 ginsenoside Rg1 on ADP-induced P2Y12 activation were examined in antagonist modes.

568

569 ***Ex vivo* ADP-induced platelet aggregation assay**

570 *Ex vivo* ADP-induced platelet aggregation assay was performed as previously
571 described[61]. Sprague-Dawley (SD) rats (300–350 g body weight) obtained from the Animal
572 Center of Chinese Academy of Medical Sciences were kept in a temperature-controlled
573 environment (24 °C) under a 12/12-h light/dark cycle, fed with normal rat chow and water ad
574 libitum. All protocols and procedures were approved by the Animal Care and Welfare
575 Committee of Institute of Materia Medica, Chinese Academy of Medical Sciences and Peking
576 Union Medical College, Beijing, China. Intravenous injection of ginsentide TP1 (10 mg/kg) or
577 oral gavage of ginsentide TP1 (3, 10, 30 mg/kg) to SD rats were conducted once daily for 3
578 days. The control rats were given 0.9 % normal saline. All *ex vivo* experiments were conducted
579 30 min after the final pre-treatment. Rats were anesthetized with 10 % chloral hydrate
580 (3 mL/kg, i.p.), and blood was collected from the abdominal aorta and anticoagulated with
581 sodium citrate (3.8 %; 1:9, *v*/*v*). Platelet-rich plasma (PRP) was obtained by centrifuging blood
582 at 1000 rpm for 10 min at room temperature. And, the remainder further centrifuged at
583 3000 rpm for 10 min to obtain platelet-poor plasma (PPP). The platelet counts of PRP were
584 adjusted to 4×10^8/mL with PPP. Platelet aggregation was determined by Born's method (Born
585 GV (1962) Aggregation of blood platelets by adenosine diphosphate and its reversal. Nature
586 194:927–929) using a four-channel aggregometer (LBY-NJ4, Beijing Precil Instrument
587 Co.Ltd., China). 300 μL PRP was placed in a cuvette and stirred with rotor at 37 °C for 5 min.
588 ADP (2.5 or 5 μM) was added to initiate platelet aggregation. Platelet aggregation was

589 determined by calibrating the equipment at 0 % light transmission for PRP and at 100 % for
590 PPP. All experiments were conducted within 2 h of blood collection. The percentage of platelet
591 aggregation was determined by optical density. The aggregation curve was recorded for 5 min,
592 and the peak value was received and served as the maximal aggregation (MAG). Inhibition%
593 of platelet aggregation was calculated from the formula: inhibition% = (MAG of
594 control − MAG of tests) / MAG of control × 100 %.
595
596 ***In vivo* acute pulmonary thrombosis**
597 The anti-thrombotic effects of ginsentide TP1 was studied using an *in vivo* acute
598 thrombotic mouse model[62] conducted by Thousand Dimensions (Beijing) Science and
599 Technology Co., Ltd, Beijing, China, as a service contract. Male Institute of Cancer Research
600 (ICR) mice (23-25 g body weight) were purchased from Beijing HFK bioscience CO.,LTD,
601 Beijing, China. Briefly, Animals were randomly divided into 6 groups: sham group (N=5) ,
602 control group (N=8), clopidogrel group (50 mg/kg) (N=7), aspirin group (100 mg/kg) (N=9),
603 ginsentide TP1 group (10 mg/kg) (N=7), and ginsentide TP1 group (30 mg/kg) (N=7). Animals
604 in each group were given the corresponding dose once a day at a dose volume of 10 mL/kg for
605 3 consecutive days, and the control group was given the corresponding volume of distilled
606 water. Animals received a saline injection containing rat tail collagen (1.5 mg/kg) and
607 epinephrine (0.5 mg/kg) via tail vein 1 h after dosing on Day 3. After intravenous injection for
608 15 s, the death of animals were recorded. 30 min after tail intravenous injection, the animals
609 were sacrificed and their lungs were dissected. The dissected lungs were washed with saline,
610 dried with filter paper, and weighed. In the sham group, tail vein injection was not performed
611 and the animals were sacrificed three days later for lung measurement. The statistical indicators
612 were lung coefficient and mortality. Lung coefficient= Lung tissue weight/Body weight*100%
613

614 **Forced swimming test**

615 Male ICR mice (220-240 mg body weight) obtained from the Animal Center of Chinese
616 Academy of Medical Sciences were kept in a temperature-controlled environment (24 °C)
617 under a 12/12-h light/dark cycle, with food and water available. The animals were given 1 week
618 to acclimatize to the housing conditions before the beginning of the experiments. All protocols
619 and procedures were approved by the Animal Care and Welfare Committee of Institute of
620 Materia Medica, Chinese Academy of Medical Sciences and Peking Union Medical College,
621 Beijing, China. The Forced Swimming Test (FST) was performed as previously described[63, 64].
622 The animals were divided into control and three experimental groups as follows: vehicle-
623 control (0.9% physiological saline) (N=14), fluoxetine (20 mg/kg) (N=13), ginsentide TP1 (10
624 mg/kg) (N=6), ginsentide TP1 (30 mg/kg) (N=13). All treatments were administered by oral
625 (p.o.) gavage in a volume of 10 mL/kg body weight. Fluoxetine and ginsentide TP1 were
626 administered to mice 30 min and 60 min before and after the FST, respectively. Mice were
627 individually placed in a glass cylinder (20 cm in height, 14 cm in diameter) filled 10 cm high
628 with water (25 ± 2 °C). All animals were forced to swim for 6 min, and the duration of
629 immobility was observed and measured during the final 4 min interval of the test. Immobility
630 period was regarded as the time spent by the mouse floating in the water without struggling
631 and making only those movements necessary to keep its head above the water. The test sessions
632 were recorded by a video camera and scored by an observer blind to treatment.

633

634 **Tail suspension test**

635 Male ICR mice (220-240 mg body weight) obtained from the Animal Center of Chinese
636 Academy of Medical Sciences were kept in a temperature-controlled environment (24°C)
637 under a 12/12-h light/dark cycle, with food and water available. The animals were given 1 week
638 to acclimatize to the housing conditions before the beginning of the experiments. All protocols

639 and procedures were approved by the Animal Care and Welfare Committee of Institute of
640 Materia Medica, Chinese Academy of Medical Sciences and Peking Union Medical College,
641 Beijing, China. The Tail Suspension Test (TST) was conducted as previously described[52]. The
642 animals were divided into control and three experimental groups as follows: vehicle-control
643 (0.9% physiological saline) (N=13), fluoxetine group (20 mg/kg) (N=13), ginsentide TP1
644 group (10 mg/kg) (N=20), ginsentide TP1 group (30 mg/kg) (N=12). All treatments were
645 administered by oral (p.o.) gavage in a volume of 10 mL/kg body weight. Fluoxetine and
646 ginsentide TP1 were administered to mice a day before as well as 30 min and 60 min,
647 respectively, before the TST. Briefly, mice were individually suspended by tail with a clamp
648 (1 cm from the tip of the end) in a box (25 × 25 × 30 cm) with the head 5 cm from the bottom.
649 Testing was carried out in a darkened room with minimal background noise. A mouse was
650 suspended for a total of 6 min, and the duration of immobility was recorded during the final 4
651 min interval of the test. Mice were considered immobile only when they hung passively and
652 completely motionless. The test sessions were recorded by a video camera and scored by an
653 observer blind to treatment.
654
655 **Statistics**
656 Statistical comparisons were performed using GraphPad Version 8.2.1 (US). Data were
657 analyzed using one-way analysis of variance (ANOVA) followed by Newman-Keuls *post hoc*
658 tests. Data were expressed as mean±S.D. and $p<0.05$ was considered to be statistically
659 significant.
660
661 **Data Availability Section**
662 The affinity-enriched mass spectrometry data and Mascot search files generated in this
663 study has been deposited in the ProteomeXchange Consortium

(http://proteomecentral.proteomexchange.org) via the jPOSTrepo (Japan ProteOme STandard Repository) partner repository[65] under the accession codes of PXD039905 and JPST001994, respectively.

AUTHOR INFORMATION

Corresponding Author

* Corresponding author: Professor James P. Tam, School of Biological Sciences, Nanyang Technological University, 60 Nanyang Drive, 637551, Singapore

Email: JPTam@ntu.edu.sg

Author contributions

‡These authors contributed equally.

Competing interests

The authors declare that the research was conducted in the absence of any commercial or financial relationships that could be construed as a potential conflict of interest.

References

1. Attele AS, Wu JA, Yuan C-S. Ginseng pharmacology: multiple constituents and multiple actions. *Biochemical pharmacology* **58**, 1685-1693 (1999).

2. Kim HJ, Kim P, Shin CY. A comprehensive review of the therapeutic and pharmacological effects of ginseng and ginsenosides in central nervous system. *Journal of ginseng research* **37**, 8 (2013).

3. Lu J-M, Yao Q, Chen C. Ginseng compounds: an update on their molecular mechanisms and medical applications. *Current vascular pharmacology* **7**, 293-302 (2009).

4. Irfan M, Kwak Y-S, Han C-K, Hyun SH, Rhee MH. Adaptogenic effects of Panax ginseng on modulation of cardiovascular functions. *Journal of Ginseng Research* **44**, 538-543 (2020).

5. Li TS. Asian and American ginseng—a review. *HortTechnology* **5**, 27-34 (1995).

6. Shin B-K, Kwon SW, Park JH. Chemical diversity of ginseng saponins from Panax ginseng. *Journal of ginseng research* **39**, 287-298 (2015).

7. Ru W, *et al.* Chemical constituents and bioactivities of Panax ginseng (CA Mey.). *Drug discoveries & therapeutics* **9**, 23-32 (2015).

8. Shi Z-Y, Zeng J-Z, Wong AST. Chemical structures and pharmacological profiles of ginseng saponins. *Molecules* **24**, 2443 (2019).

9. Ratan ZA, *et al.* Pharmacological potential of ginseng and its major component ginsenosides. *Journal of ginseng research* **45**, 199-210 (2021).

10. Mohanan P, Subramaniyam S, Mathiyalagan R, Yang D-C. Molecular signaling of ginsenosides Rb1, Rg1, and Rg3 and their mode of actions. *Journal of Ginseng Research* **42**, 123-132 (2018).

11. Gao Y, *et al.* Ginsenoside Rg1 prevent and treat inflammatory diseases: A review. *International immunopharmacology* **87**, 106805 (2020).

12. Kim JH, Yi Y-S, Kim M-Y, Cho JY. Role of ginsenosides, the main active components of Panax ginseng, in inflammatory responses and diseases. *Journal of ginseng research* **41**, 435-443 (2017).

13. Ma X, *et al.* Cardioprotective Effects and Mechanisms of Saponins on Cardiovascular Disease. *Natural Product Communications* **17**, 1934578X221147404 (2022).

14. Loo S, *et al.* Anti-fungal Hevein-like peptides biosynthesized from quinoa cleavable hololectins. *Molecules* **26**, 5909 (2021).

15. Loo S, Tay SV, Kam A, Lee W, Tam JP. Hololectin interdomain linker determines asparaginyl endopeptidase-mediated maturation of antifungal hevein-like peptides in oats. *Frontiers in Plant Science* **13**, (2022).

16. Loo S, Kam A, Li BB, Feng N, Wang X, Tam JP. Discovery of hyperstable noncanonical plant-derived epidermal growth factor receptor agonist and analogs. *Journal of Medicinal Chemistry* **64**, 7746-7759 (2021).

17. Kam A, Loo S, Fan J-S, Sze SK, Yang D, Tam JP. Roseltide rT7 is a disulfide-rich, anionic, and cell-penetrating peptide that inhibits proteasomal degradation. *Journal of Biological Chemistry* **294**, 19604-19615 (2019).

18. Tam JP, Nguyen GK, Loo S, Wang S, Yang D, Kam A. Ginsentides: cysteine and glycine-rich peptides from the ginseng family with unusual disulfide connectivity. *Scientific reports* **8**, 1-15 (2018).

19. Veith I. *The yellow emperor's classic of internal medicine*. Univ of California Press (2015).

20. Yang S. *The divine farmer's materia medica: a translation of the Shen Nong Ben Cao Jing*. Blue Poppy Enterprises, Inc. (1998).

21. Nugent-Head J. The First Materia Medica: The Shen Nong Ben Cao Jing. *Journal of Chinese Medicine*, (2014).

22. Curran J. Medical classics: The Yellow Emperor's Classic of internal Medicine. *BMJ: British Medical Journal* **336**, 777 (2008).

23. Zhongjing Z. *Treatise of Febrile Diseases Caused by Cold (Shanghan Lun)*. New World Press (1986).

24. ion Center RR. A review of the properties and clinical effects of ginseng. *American Journal of Chinese Medicine* **1**, 263-270 (1973).

25. Kiefer DS, Pantuso T. Panax ginseng. *American family physician* **68**, 1539-1542 (2003).

26. Ellis JM, Reddy P. Effects of Panax ginseng on quality of life. *Annals of pharmacotherapy* **36**, 375-379 (2002).

27. Coleman C, Hebert J, Reddy P. The effects of Panax ginseng on quality of life. *Journal of clinical pharmacy and therapeutics* **28**, 5-15 (2003).

28. Todorova V, Ivanov K, Delattre C, Nalbantova V, Karcheva-Bahchevanska D, Ivanova S. Plant adaptogens—history and future perspectives. *Nutrients* **13**, 2861 (2021).

29. Kam A, Loo S, Dutta B, Sze SK, Tam JP. Plant-derived mitochondria-targeting cysteine-rich peptide modulates cellular bioenergetics. *Journal of Biological Chemistry* **294**, 4000-4011 (2019).

30. Gillis CN. Panax ginseng pharmacology: a nitric oxide link? *Biochemical pharmacology* **54**, 1-8 (1997).

31. Kim J-H. Pharmacological and medical applications of Panax ginseng and ginsenosides: a review for use in cardiovascular diseases. *Journal of ginseng research* **42**, 264-269 (2018).

32. Chen X. Cardiovascular protection by ginsenosides and their nitric oxide releasing action. *Clinical and experimental pharmacology and physiology* **23**, 728-732 (1996).

33. Dimmeler S, Fleming I, Fisslthaler B, Hermann C, Busse R, Zeiher AM. Activation of nitric oxide synthase in endothelial cells by Akt-dependent phosphorylation. *Nature* **399**, 601-605 (1999).

34. Michell B*, et al.* The Akt kinase signals directly to endothelial nitric oxide synthase. *Current biology* **9**, 845-S841 (1999).

35. Zhang Y*, et al.* PI3K/AKT signaling pathway plays a role in enhancement of eNOS activity by recombinant human angiotensin converting enzyme 2 in human umbilical vein endothelial cells. *International journal of clinical and experimental pathology* **7**, 8112 (2014).

36. Brotman DJ, Golden SH, Wittstein IS. The cardiovascular toll of stress. *The Lancet* **370**, 1089-1100 (2007).

37. Kjeldsen SE, Rostrup M, Moan A, Mundal HH, Gjesdal K, Eide IK. The sympathetic nervous system may modulate the metabolic cardiovascular syndrome in essential hypertension. *Journal of cardiovascular pharmacology* **20**, S32-S39 (1992).

38. Rameshrad M, Babaei H, Azarmi Y, Fouladi DF. Rat aorta as a pharmacological tool for in vitro and in vivo studies. *Life sciences* **145**, 190-204 (2016).

39. Black PH, Garbutt LD. Stress, inflammation and cardiovascular disease. *Journal of psychosomatic research* **52**, 1-23 (2002).

40. Marchio P, Guerra-Ojeda S, Vila JM, Aldasoro M, Victor VM, Mauricio MD. Targeting early atherosclerosis: a focus on oxidative stress and inflammation. *Oxidative medicine and cellular longevity* **2019**, (2019).

41. Hulsmans M, Holvoet P. The vicious circle between oxidative stress and inflammation in atherosclerosis. *Journal of cellular and molecular medicine* **14**, 70-78 (2010).

42. Ng T. Pharmacological activity of sanchi ginseng (Panax notoginseng). *Journal of Pharmacy and Pharmacology* **58**, 1007-1019 (2006).

43. Xue Q*, et al.* Functional roles and mechanisms of ginsenosides from Panax ginseng in atherosclerosis. *Journal of ginseng research* **45**, 22-31 (2021).

44. Lee CH, Kim J-H. A review on the medicinal potentials of ginseng and ginsenosides on cardiovascular diseases. *Journal of ginseng research* **38**, 161-166 (2014).

45. Irfan M, Kim M, Rhee MH. Anti-platelet role of Korean ginseng and ginsenosides in cardiovascular diseases. *Journal of ginseng research* **44**, 24-32 (2020).

46. Jin YR*, et al.* Antithrombotic and antiplatelet activities of Korean red ginseng extract. *Basic & Clinical Pharmacology & Toxicology* **100**, 170-175 (2007).

47. Yu JY*, et al.* Antiplatelet and antithrombotic activities of Korean Red Ginseng. *Archives of pharmacal research* **29**, 898-903 (2006).

48. Gul H, Jamshed A, Jabeen Q. Pharmacological Investigation of Asphodelus tenuifolius Cav. for its potential against thrombosis in experimental models. *Dose-Response* **20**, 15593258221127566 (2022).

49. Hammen C. Stress and depression. *Annu Rev Clin Psychol* **1**, 293-319 (2005).

50. Robles TF, Glaser R, Kiecolt-Glaser JK. Out of balance: A new look at chronic stress, depression, and immunity. *Current Directions in Psychological Science* **14**, 111-115 (2005).

51. Petit-Demouliere B, Chenu F, Bourin M. Forced swimming test in mice: a review of antidepressant activity. *Psychopharmacology* **177**, 245-255 (2005).

52. Steru L, Chermat R, Thierry B, Simon P. The tail suspension test: a new method for screening antidepressants in mice. *Psychopharmacology* **85**, 367-370 (1985).

53. Kitts D, Hu C. Efficacy and safety of ginseng. *Public health nutrition* **3**, 473-485 (2000).

54. Kemeny ME. The psychobiology of stress. *Current directions in psychological science* **12**, 124-129 (2003).

55. McCarty R. The fight-or-flight response: A cornerstone of stress research. In: *Stress: Concepts, cognition, emotion, and behavior*). Elsevier (2016).

56. Chu B, Marwaha K, Sanvictores T, Ayers D. Physiology, stress reaction. In: *StatPearls [Internet]*). StatPearls Publishing (2021).

57. Loo S, Kam A, Xiao T, Nguyen GK, Liu CF, Tam JP. Identification and characterization of roseltide, a knottin-type neutrophil elastase inhibitor derived from Hibiscus sabdariffa. *Scientific reports* **6**, 39401 (2016).

58. Loo S, Kam A, Xiao T, Tam JP. Bleogens: cactus-derived anti-Candida cysteine-rich peptides with three different precursor arrangements. *Frontiers in plant science* **8**, 2162 (2017).

59. Yeung Y-G, Stanley ER. A solution for stripping antibodies from polyvinylidene fluoride immunoblots for multiple reprobing. *Analytical biochemistry* **389**, 89-91 (2009).

60. Lüscher T, Vanhoutte PM. Endothelium-dependent contractions to acetylcholine in the aorta of the spontaneously hypertensive rat. *Hypertension* **8**, 344-348 (1986).

61. Yang H, Xu S, Li J, Wang L, Wang X. Potassium 2-(1-hydroxypentyl)-benzoate inhibits ADP-induced rat platelet aggregation through P2Y 1-PLC signaling pathways. *Naunyn-Schmiedeberg's archives of pharmacology* **388**, 983-990 (2015).

62. Chen G-L*, et al.* Chitosan/Alginate Nanoparticles for the Enhanced Oral Antithrombotic Activity of Clam Heparinoid from the Clam Coelomactra antiquata. *Marine Drugs* **20**, 136 (2022).

63. Porsolt R, Bertin A, Jalfre M. Behavioral despair in mice: a primary screening test for antidepressants. *Archives internationales de pharmacodynamie et de therapie* **229**, 327-336 (1977).

64. Bourin M, Mocaër E, Porsolt R. Antidepressant-like activity of S 20098 (agomelatine) in the forced swimming test in rodents: involvement of melatonin and serotonin receptors. *Journal of Psychiatry and Neuroscience* **29**, 126-133 (2004).

65. Okuda S*, et al.* jPOSTrepo: an international standard data repository for proteomes. *Nucleic acids research* **45**, D1107-D1111 (2017).